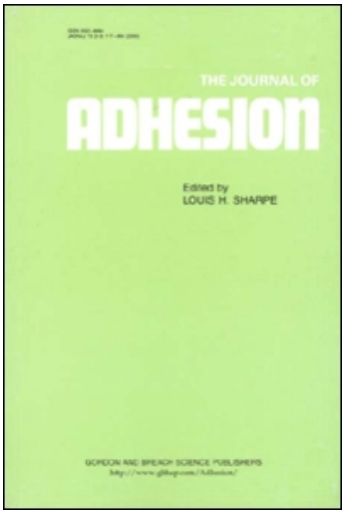

The Journal of Adhesion
Publication details, including instructions for authors and subscription information:
http://www.informaworld.com/smpp/title~content=t713453635

New Organic Montmorillonite: Application to Room-Temperature Vulcanized Silicone Rubber Adhesive System

Jincheng Wang[a]; Yuehui Chen[a]; Qiqi Jin[a]
[a] College of Chemistry and Chemical Engineering, Shanghai University of Engineering Science, Shanghai, China

To cite this Article Wang, Jincheng , Chen, Yuehui and Jin, Qiqi(2006) 'New Organic Montmorillonite: Application to Room-Temperature Vulcanized Silicone Rubber Adhesive System', The Journal of Adhesion, 82: 4, 389 — 405
To link to this Article: DOI: 10.1080/00218460600683910
URL: http://dx.doi.org/10.1080/00218460600683910

The Journal of Adhesion, 82:389–405, 2006

ISSN: 0021-8464 print/1545-5823 online
DOI: 10.1080/00218460600683910

Taylor & Francis
Taylor & Francis Group

New Organic Montmorillonite: Application to Room-Temperature Vulcanized Silicone Rubber Adhesive System

Jincheng Wang
Yuehui Chen
Qiqi Jin
College of Chemistry and Chemical Engineering,
Shanghai University of Engineering Science, Shanghai, China

Montmorillonite clay was modified with a new intercalation agent and was added with different amounts to the room-temperature-vulcanizing silicone rubber (RTV-SR) adhesive system. Both the reinforcing and compatibilizing performance of the filler were investigated using physicomechanical properties, wide angle X-ray diffraction (WAXD), Fourier transform infrared (FTIR) spectroscopy, and transmission electron microscopy (TEM). There was a remarkable increase of cohesive strength and tensile and thermal properties with the organic montmorillonite (OMMT) loading up to 10 parts per hundred of resin by weight (phr). It was proposed that the nanoreinforcing effect caused by the well-dispersed silicate layers may reduce the amount and size of voids and increase the length of the crack spread path during lap shear testing.

Keywords: Cohesive mechanism; Organic montmorillonite; Properties; Room-temperature-vulcanized silicone rubber

INTRODUCTION

Room-temperature-vulcanized silicone rubber (RTV-SR) adhesive is one of the most important types of high-temperature-resistant synthetic adhesives, with excellent thermal stability, low-temperature toughness, and electrical-insulating properties. It has been extensively used in electrical-insulating products, sealing products, and so forth. However, it is of low strength compared with other organic

Received 31 August 2005; in final form 7 March 2006.
Address correspondence to Wang Jincheng, Room 302, 2 Hao, 383 Nong, Yuanping Road, Zhabei District, Shanghai 200436, China. E-mail: wjc406@263.net

adhesives because of the weaker interaction between polysiloxane macromolecules [1,2].

Considerable efforts have been directed at improving the mechanical properties of silicone rubber: on one hand, modification of the molecular structure by chemical cross links, such as replacing some methyl groups of polydimethylsiloxane with vinyl groups, using vinyl-terminated methylvinylpolysiloxane as gum, or adding methylene or phenylene to the main chains; and on the other hand, using physical means, such as incorporation of mineral fillers by alternative novel techniques, a sol-gel process to precipitate particles such as silica into the elastomeric matrix [3–6], and the use of colloidal silica to generate spherical nanoparticles through the Stöber process [7,8]. The main aims for reinforcement by fillers are the enhancement of adhesive strength, tensile strength, modulus, abrasion resistance, or reducing cost [9].

Currently, most silicone rubber adhesives are reinforced by aerosilica, which is more expensive than other fillers. Aerosilica, with a very small particle size (5–20 nm), aggregates readily and is difficult to disperse in the adhesive matrix. We are not aware of any case that pyrophoric fumed silica can cause silicosis, but finely divided quartz does cause harm [10]. Because of its high price, easy agglomeration, and harm to workers' health, researchers focused on the development of other reinforcing fillers such as organic montmorillonite (OMMT) to replace aerosilica [11–13].

In this article, we describe a specific RTV-SR adhesive using a new type of OMMT. The cohesive, tensile, and thermal properties of the adhesive with different amounts of OMMT incorporated were researched and compared. A combination of Fourier transform infrared (FTIR) spectroscopy, wide-angle X-ray diffraction (WAXD), and transmission electron microscopy (TEM) studies demonstrated that the molecular structure of RTV-SR was somewhat disrupted by the presence of the OMMT. Results showed that the presence of 10 phr of OMMT in the RTV-SR matrix can greatly improve the cohesive strength and other properties because of the nanoeffect of silicate layers of OMMT in the system.

EXPERIMENTAL

RTV-SR (consisting of two components: component A, hydroxyl containing base rubber, $H(O-Si(CH_3)_2)_nOH$, the number-average molar mass ($\overline{M_n}$) is 70,000; component B, alkoxy silane cross-linker, $(C_2H_5O)_4Si$, and tin dibutyl dilauric acid catalyst; molar ratio: component A:B = 10:1) was supplied by Shanghai Rubber Product Institute (China).

Na^+-montmorillonite (MMT, $Na_{0.7}(Al_{3.3}\ Mg_{0.7})Si_8O_{20}(OH)_4 \cdot nH_2O$) with a cation-exchange capacity of 115 meq per 100 g, industrial grade, was obtained from Zhejiang Fenghong Clay Company (China). Aerosilica, industrial grade, was bought from Shanghai Zhonghai Chemical Company (China). Dihydroxyethyl dodecyl trimethyl ammonium chloride (DDTAC), chemically pure, was received from Zhejiang Chemical Agent Company (China).

A 500-mL round-bottomed, three-necked flask equipped with a mechanical stirrer, thermometer, and condenser with drying tube was used as a reactor. MMT (10 g) was gradually added to a previously prepared solution of DDTAC (3.52 g), which was dissolved in 120 mL of ethanol/water mixture (1:1, w/w), and the resultant suspension was vigorously stirred at 75–80°C for 2 h. The treated MMT was repeatedly washed by deionized water. The filtrate was titrated with 0.1 N $AgNO_3$ until no precipitate of AgCl was formed, to ensure the complete removal of chloride ions. The filter cake was then placed in a vacuum oven at 80°C for 12 h to dry. The dried cake was ground to obtain the OMMTs.

Different amounts of OMMT (0, 5, 10, 15, 20 wt.%) were mixed with 100 g of hydroxyl containing base rubber. After vigorous stirring at room temperature for 3 h, the mixture was then blended with 10 g of alkoxy silane cross-linker, including tin dibutyl dilauric acid catalyst, and stirred for 0.5 h. Thus, the novel transparent adhesives were obtained.

Figure 1 shows the specimen of lap shear strength that was tested at a separation rate of 5 ± 1 mm/min according to GB 7124-86 in a XL-250A tensile strength tester (guaugzhou Instrument Co., China). The 100% copper test substrates with a prescribed size, $100 \times 25 \times 2 \times$ mm^3, were first burnished by sand paper, then washed and cleaned with acetone, and lastly kept in a controlled atmosphere of $50 \pm 5\%$ relative humidity and 23 ± 2°C for 2 h prior to test. The adhesive was coated with a thickness of 20–25 μm between the two copper plates, and the lapped length was 12.5 mm (shown in the Figure 1b). The sandwiched specimens were then cured at 25°C for 24 h before adhesion testing. The results reported are the average of five samples.

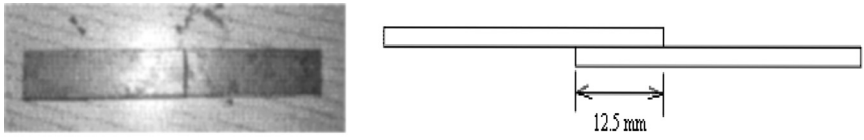

FIGURE 1 Specimen of lap shear strength: (a) front view and (b) side view.

Films of the RTV-SR/OMMT mixture were prepared by molding. Curing was conducted at room temperature (20°C) for 24 h, after which an elastic film was obtained. Dumbbells were die-cut from the films, and the tensile tests were carried out with an Instron Model 4204 instrument (Instron, High Wycombe, UK) at room temperature with a crosshead speed of 500 mm/min. All measurements were repeated five times, and an average was determined.

Thermogravimetric analysis (TGA) of MMT, OMMT, and RTV-SR and its nanocomposites was carried out at 10°C/min under air (flow rate $5 \times 10^{-7}\,m^3/s$, air liquid grade) using a Universal V3.8B TA microbalance (TA Instruments, New Castle, DE, USA). In each case, the mass of the sample used was fixed at 10 mg, and the samples were positioned in open vitreous silica pans. The precision of the temperature measurements was 1°C over the whole range of temperatures.

To measure the change of gallery distance of OMMT and RTV-SR/OMMT before and after intercalation, WAXD was performed at room temperature with a Rigaku D-Max/400 (Japan) X-ray diffractometer (Rigacu, Tokyo, Japan). The X-ray beam was nickel-filtrated Cukα ($\lambda = 0.154$ nm) radiation operated at a generator voltage of 50 kV and a generator current of 100 mA, and the diffraction data were obtained from 1 to 10° (2θ) at a rate of 2°/min. Samples were pellets with a smooth surface and a dimension of 10 (width) × 10 (height) × 1 (thickness) mm^3.

FTIR spectra were recorded on a Nicolet 170SX FTIR (Thermo Electron Corp., Madison, WI, USA) in the range 4000–600 cm^{-1}, and the resolution was 2 cm^{-1}. Samples were ground and mixed with KBr to form pellets. Sixty-four scans were necessary to obtain spectra with good signal-to-noise ratios.

TEM images were taken using a H-800 instrument (Hitachi Co., Tokyo, Japan) operated at an acceleration voltage of 200 kV and beam current 15 μA under low-dose conditions and at a magnification of about 10,000×, to minimize beam damage. Specimens of the RTV-SR/OMMT nanocomposites were refrigerated at −130°C in a liquid nitrogen trap, and 80-to-100-nm-thick sections were prepared by a cryogenic ultramicrotome system with a diamond knife in a direction normal to the plane of the films. Subsequently, a layer of carbon about 3 nm thick was deposited on these slices, on 200 mesh copper nets for TEM observation.

RESULTS AND DISCUSSION

Table 1 shows the average lap shear strength of the pure RTV-SR, RTV-SR/OMMT, and RTV-SR/aerosilica adhesives. In all cases, the

shear strength of the adhesives filled with different amounts of OMMT was a much higher than that of the pure system. The shear strength was improved to 0.91 MPa and was increased 3.8 times with the OMMT loading at 10 phr. It was also observed that when the OMMT amount increased to 15 and 20 phr, the shear strength decreased, which was probably caused by the aggregates of the OMMT in the adhesives. Later in the article we show this by WAXD. The shear strength of RTV-SR/aerosilica adhesives increased with increasing aerosilica content. In all these systems, the fracture mode was cohesive failure (*i.e.*, the failure occurred in the RTV-SR films). It can be concluded that the lap shear strength of RTV-SR/OMMT-10 adhesive was almost equal to that of RTV-SR/aerosilica-20 composite [14].

The tensile properties of the different adhesives are also compared in Table 2. Compared with that of the pure RTV-SR and RTV-SR/aerosilica systems, RTV-SR/OMMT composites showed a higher tensile strength and elongation at break. Wang *et al*. [11] synthesized a silicone rubber/OMMT hybrid by means of solution and melt mixing. The mechanical properties of the hybrid were compared with those of the silicone rubber filled with aerosilica. The results proved that OMMT could improve the tensile strength from 0.20 MPa to 1.51 MPa, which was close to that of aerosilica-filled silicone composite. Obviously, in this article, the tensile strength of RTV-SR/OMMT-10 was 1.64 MPa and was about 3.9 times as high as that of the pure RTV-SR. The elongation at break also showed a remarkable enhancement. This shows the excellent reinforcing ability of the OMMT being used. When the amount of OMMT increased more than 10 phr, the tensile strength decreased, which may be caused by the negative effect of the OMMTs that are not well intercalated or dispersed. Also, it can be seen from the table that the tensile properties of RTV-SR/

TABLE 1 Lap Shear Strength of Pure RTV-SR, RTV-SR/OMMT, and RTV-SR/Aerosilica Adhesives

Materials	Lap shear strength/MPa
Pure RTV-SR	0.24
RTV-SR/OMMT-5	0.39
RTV-SR/OMMT-10	0.91
RTV-SR/OMMT-15	0.69
RTV-SR/OMMT-20	0.48
RTV-SR/aerosilica-5	0.32
RTV-SR/aerosilica-10	0.48
RTV-SR/aerosilica-15	0.64
RTV-SR/aerosilica-20	0.81

TABLE 2 Tensile Properties of Pure RTV-SR, RTV-SR/OMMT, and RTV-SR/Aerosilica Adhesives

Materials	Tensile strength/MPa	Elongation at break/%
Pure RTV-SR	0.42	95
RTV-SR/OMMT-5	1.22	142
RTV-SR/OMMT-10	1.64	155
RTV-SR/OMMT-15	1.43	135
RTV-SR/OMMT-20	1.10	121
RTV-SR/aerosilica-5	1.11	128
RTV-SR/aerosilica-10	1.25	139
RTV-SR/aerosilica-15	1.40	150
RTV-SR/aerosilica-20	1.56	163

OMMT-10 were nearly the same as that of RTV-SR/aerosilica-20 composite.

TGA under an air atmosphere was applied to evaluate the thermal stability of MMT, OMMT, pure RTV-SR, and the selected RTV-SR adhesive composites, and their results are shown in Figure 2. MMT first lost weight in the temperature range of 45–100°C. The weight loss was about 10%, corresponding to the removal of water from the interlayers of coordinated Na^+. For OMMT, the weight loss in this temperature range was about 3%, which was due to the smaller amount of water absorbed by the intercalation agent, DDTAC [15]. The weight loss in the temperature range of 100–400°C for MMT was about 2%, which can be attributed to the decomposition of hydrogen-bonded water molecules and some of the hydroxyl groups from the tetrahedral sheets [16]. The weight loss in this temperature range of OMMT was about 20%, which is explained mainly by the decomposition and oxidation of intercalated ammonium and partly from the adsorbed water molecules [17]. The weight loss in the temperature range above 400°C for MMT and OMMT should both be associated with the dehydroxylation of MMT [18]. The characteristic thermal parameters for the degradation of the pure RTV-SR and the selected RTV-SR composites are initial, center temperature and char residue of thermal degradation, and the results are summarized in Table 3. The first increasing and the later decreasing of initial degradation temperature was probably caused by the increasing amount of organic small molecules of the intercalation agent. Similarly, the center temperature also has this trend. The nonlinear effect on the initiation and center temperature may result from the following integrated reasons. First, the addition of OMMT can add inorganic MMT silicate layers to the systems and thus can increase their thermal stability. The greater the amounts

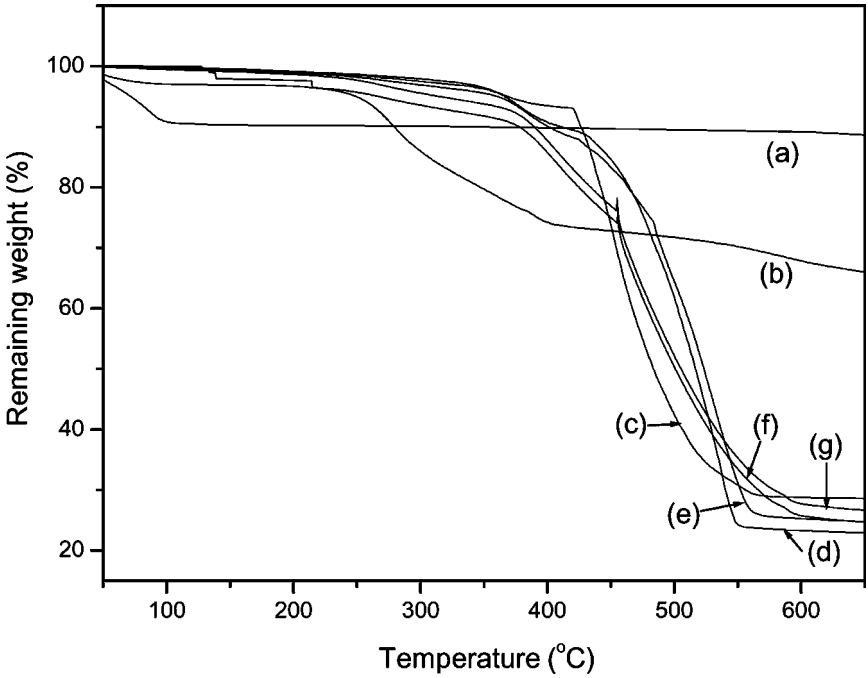

FIGURE 2 TGA curves of (a) MMT, (b) OMMT, (c) pure RTV-SR, (d) RTV-SR/OMMT-5, (e) RTV-SR/OMMT-10, (f) RTV-SR/OMMT-20, and (g) RTV-SR/aerosilica-20.

of OMMT, the higher the degradation temperatures; second, the incorporation of OMMT can add the organic intercalation agent to the composites and thus may decrease their corresponding temperatures because of its easy degradation. The higher the amount of OMMT, the lower the temperatures. The highest initial and center temperature of RTV-SR/OMMT-10 resulted from the highest retardation

TABLE 3 TGA Data of Pure RTV-SR, RTV-SR/OMMT, and RTV-SR/Aerosilica Adhesives

Materials	Char residue/%	Initial temperature of thermal degradation/°C	Center temperature of thermal degradation/°C
Pure RTV-SR	30	335	435
RTV-SR/OMMT-5	25	348	446
RTV-SR/OMMT-10	27	354	485
RTV-SR/OMMT-20	28	293	441
RTV-SR/aerosilica-20	27	350	479

effect of the silicate layers and the least side effect of the intercalation agent on the silicone rubber molecular chains. The more chains are restricted by the silicate layers, the higher the temperatures. This also confirmed the best reinforcing effect in RTV-SR/OMMT-10 composite. On the other hand, the amount of char residue was decreased with the addition of the OMMT in the composites. In our opinion, there are at least two factors that may influence the char residue of the composites. First, the introduction of well-dispersed OMMT can lessen the heat transport and improve the thermal stability of the composites. Second, the OMMT itself contains some low-molecular-weight molecules that are easy to decompose at low temperatures. The decomposition products will be released, and too many of them are sure to impair the thermal stability of the composites. The decreasing of char residue for the 5, 10, and 20 phr OMMT-filled composites may also be attributed to the integrated effect of these two factors. In the presence of 20 phr aerosilica, the characteristic degradation temperatures and the char residue of the RTV-SR adhesive were relatively lower than those of the AL-SR/OMMT-10 adhesive, which may be due to the different structures and properties of OMMT and aerosilica [19–21].

We can see that the physical and mechanical properties such as cohesive, tensile, and thermal properties were much improved by the addition of the novel OMMT. This may be influenced by the small size, suitable loading, uniform dispersion, and good compatibility of the OMMT in the silicone rubber matrix.

An important measure of the degree of dispersion of the silicate layers can be obtained by WAXD measurements. Original MMT, OMMT, and a series of WAXD patterns of the composites containing different amounts of OMMT are shown in Figure 3. Curve a, WAXD of the pure MMT, shows a characteristic peak at 6° of 2θ, which was assigned to the 001 basal reflection. In curve b, there were three peaks in the WAXD spectrum. This indicated the different degree of expansion of silicate layers in the OMMT, which was probably due to the following reasons [22]. First, the structure of the new intercalation agent could have some influence on the enlargement of silicate-layer basal spacing in the OMMT. The strong polarity of $-$OH groups, branching chains of dihydroxyethyl, and space-distributing morphology of molecular chains of this intercalation agent may influence the Coulomb force between the silicate layers and make the space between the silicate layers of the OMMT nonuniform. Second, the structure and properties of the inorganic MMT, which was produced by Zhejiang Fenghong Clay Company, may be different from other common MMTs. The Coulomb force between silicate layers of the MMT may be not uniform. No obvious peaks were observed in Figure 3c, which was

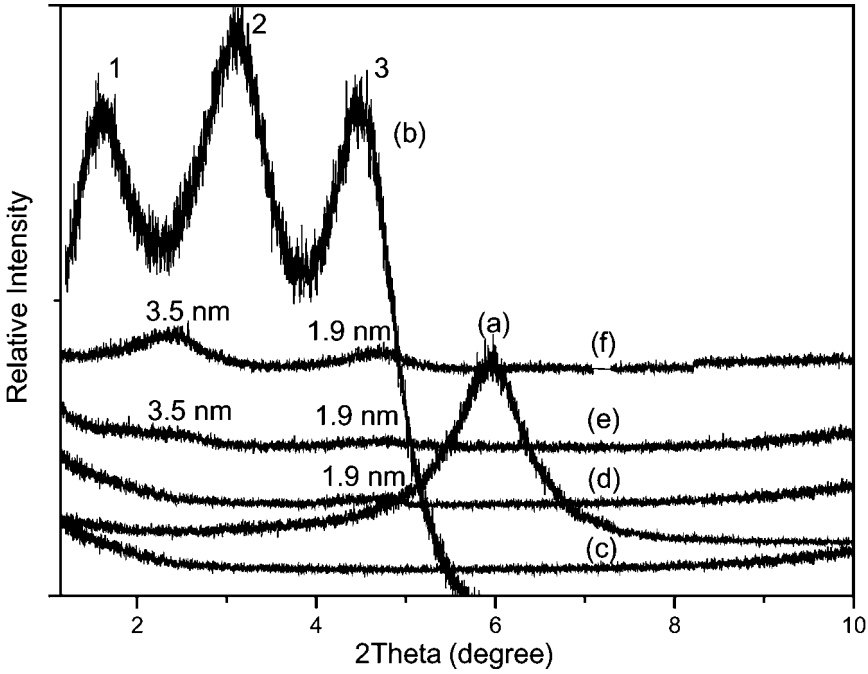

FIGURE 3 WAXD spectra of (a) Na^+-MMT, (b) OMMT, (c) pure RTV-SR, (d) RTV-SR/OMMT-5, (e) RTV-SR/OMMT-10, and (f) RTV-SR/OMMT-20.

ascribed to the original microstructure of RTV-SR. When a small amount of OMMT was incorporated (RTV-SR/OMMT-5), some peaks, which had something to do with the original silicate layer space of OMMT (shown in Figure 3b), were observed between 4–5°, indicating the existence of OMMT silicate layers dispersed in the polymer matrix. A slight peak appeared at 2.5° (d spacing = 3.5 nm), which corresponded to the expansion of the gallery space of the silicate layer by the insertion of RTV-SR polymer chains as the amount of OMMT in RTV-SR increased to 10 phr. Obvious peaks appearing at 4.6° (d spacing = 1.9 nm) in the RTV-SR/OMMT-20 composite illustrated the existence of stacked OMMT in the composites, which to some extent can demonstrate the decreased properties of this system. Also, the peaks around 5° in spectrum (e) are less obvious than those of spectrum (f), and this may be attributed to the formation of exfoliated structure in the RTV-SR/OMMT-10 system. After careful comparison of the spectra (e) and (f), a conclusion can be made that the RTV-SR-10 system is a mixture of intercalated and exfoliated nanocomposites [23–25].

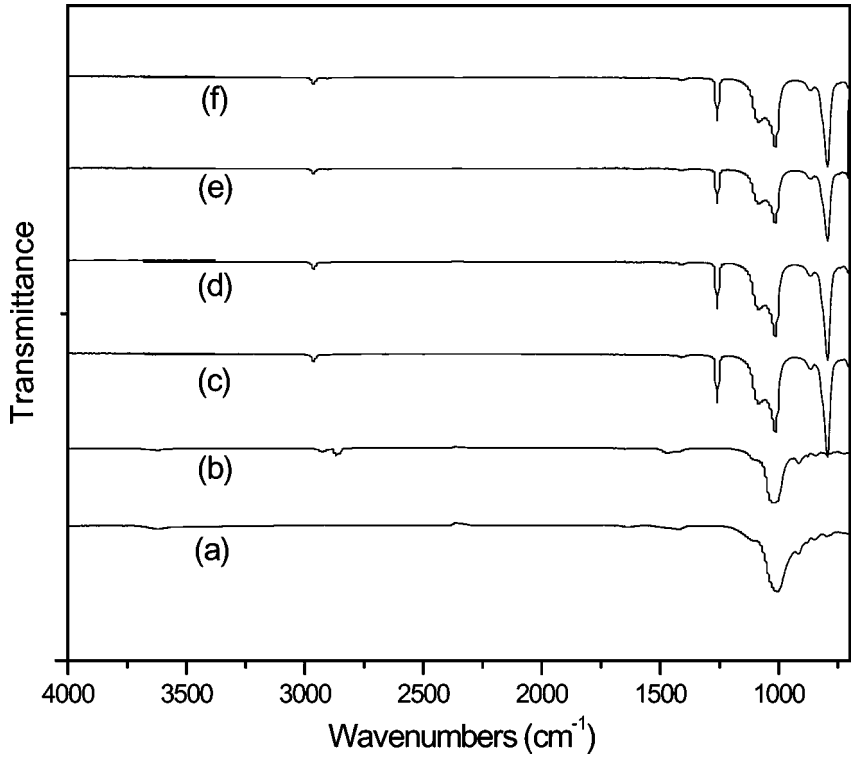

FIGURE 4 FTIR spectra of (a) MMT, (b) OMMT, (c) pure RTV-SR, (d) RTV-SR/OMMT-5, (e) RTV-SR/OMMT-10, and (f) RTV-SR/OMMT-20.

The microdomain structure of MMT, OMMT, pure RTV-SR, and different amounts of OMMT-filled RTV-SR composites were analyzed by FTIR, as shown in Figure 4. In the case of FTIR of the MMT, the 3620–3650 cm^{-1} peak was caused by the stretching of −OH, which was attributable to the physical and chemical water that exists in the Na^+-MMT. The peaks at 1030 cm^{-1} and 700 cm^{-1} resulted from the stretching vibration of Si−O and Al−O bonds in the MMT structure. In the spectrum of OMMT, in addition to the peaks that also exist in the MMT, there is the presence of new peaks at 2800–3000 cm^{-1} and 1469 cm^{-1}, which were caused by C−H stretching and bending absorptions in the organic intercalation agent. The disappearing peaks at 1640 cm^{-1}illustrated the exchanging of Na^+ cations in the MMT with the quaternary ammonium cations in the intercalation agents [26]. The positions of peaks for distinctive functional groups were almost identical both in pure RTV-SR and in RTV-SR/OMMT composites,

which means that the molecular structure of RTV-SR was not greatly affected by the presence of OMMT [27]. With the increase of OMMT amount, compared with pure RTV-SR, the intensity of absorption peaks of RTV-SR/OMMT composites is diminished between 1070–1090 cm^{-1} and 800 cm^{-1}, which may be attributed to the chemical reaction of alkoxyl silane cross-linker (component B), with the hydroxyl in the base rubber (component A), and also with −OH in DDTAC (the intercalation agent). The reason for the largest decrease of absorption peaks intensity of RTV-SR/OMMT-10 composite is probably due to the highest reacting ratio of this reaction. This reaction can lead to the partial development of Si−O−Si groups, which are fully developed in the pure RTV-SR system.

Further evidence of nanometer-scale dispersion of silicate layers in the RTV-SR/OMMT-10 composite was supported by TEM photomicrographs, as shown in Figure 5. The lower magnification micrograph, Figure 5a, shows that the OMMT layers do not fill the full volume, suggesting that the platelet tactoids of OMMT were dispersed in the RTV-SR matrix at sub-micro-sized scale. A close observation of an area of platelet tactoid at higher magnification with high-resolution TEM reveals the individual platelets of OMMT clearly separated by the polymer matrix; *i.e.*, some polymer has diffused between some of the platelets (see Figure 5b). It is evident that the morphology could be considered a mix of intercalated and exfoliated platelets; *i.e.*, there are regions where the regular stacking platelet tactoids are maintained with polymer diffusing between the platelets of OMMT (indicated by the horizontal arrows) and also regions where OMMT platelets are completely delaminated (indicated by the vertical arrows) [28].

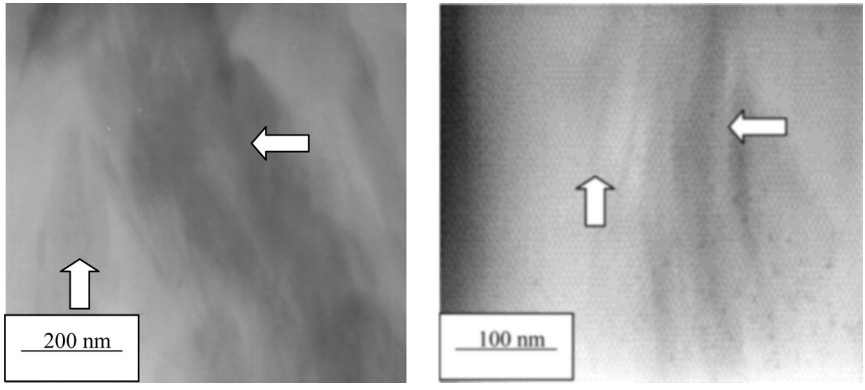

FIGURE 5 TEM images of RTV-SR/OMMT-10: (a) ×100,000 and (b)×200,000.

In the unfilled state, RTV-SR adhesives generally have poor cohesive strength and tensile properties, which can be greatly improved by the incorporation of mineral particles such as MMT. The MMT clay is a phyllosilicate mineral. Cations such as Na^+, K^+, and Ca^{2+} compensate for the negative charge that exists in the crystal lattice of each silicate layer in MMT.

To meet application requirements, it is important to monitor the interactions between MMT and the RTV-SR network by a pretreatment of the mineral. Polar molecules such as DDTAC, which can make MMT more organophilic, can penetrate between the layers and swell. The schematic depiction of the intercalation process between original MMT and DDTAC is illustrated in Figure 6. The interlayer spacing of the OMMT is so large (5.25 nm, calculated from Figure 3b) that it is greater than the extended chain length of DDTAC. The underlying mechanism may be related to the strong polarity of −OH groups, branching chains of dihydroxethyl and space-distributing morphology of molecular chains of this intercalation agent [29–32].

By increasing the interlayer spacing and making the clay more compatible with the organic polymers, the quaternary ammonium ions in DDTAC allow monomer molecules or polymer chains to diffuse between the silicate layers. The nature of this organic cation has a significant effect on the development of the exfoliation-type nanocomposites.

The schematic development of the exfoliated RTV-SR/OMMT nanocomposite is shown in Figure 7. During the stirring and drying process, alkoxyl silane not only can react with hydroxyl in the other component of RTV-SR (see Figure 8a), but also can react with −OH

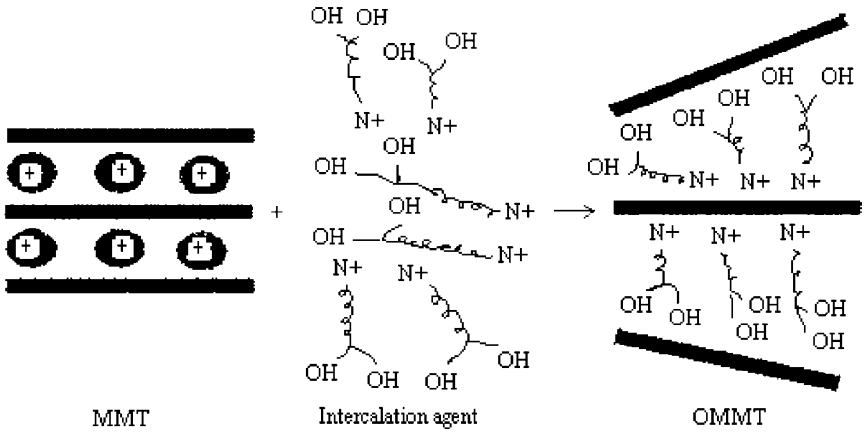

FIGURE 6 Scheme of the intercalation process of the MMT.

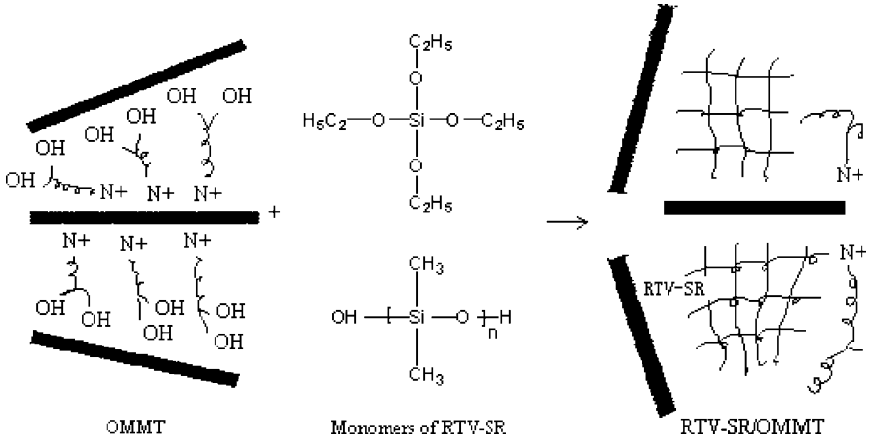

FIGURE 7 Scheme of the intercalation process between OMMT and monomers of RTV-SR.

in the intercalation agent in the OMMT (see Figure 8b), which has an important effect on the intercalation and exfoliation of the organoclay.

Two cleaned copper plates were joined with a layer of a two-component silicone resin with and without OMMT. The lap shear strength of the RTV-SR containing 10 phr OMMT is better than that of the pure RTV-SR. In all cases, the failure is cohesive (*i.e.*, in the silicone rubber film), as observed visually. The different crack characteristics of RTV-SR adhesives with and without OMMT under lap shear testing are depicted in Figure 9. The reason for the difference can be related to parameters such as bound rubber, rubber shell creation in the vicinity of each silicate layer (dark gray areas in Figure 9b), and the occlusion of rubber within the clay galleries. Thus, an increased cohesion is expected when the polymer matrix is filled with well-dispersed OMMT silicate layers.

The failure of the two kinds of adhesive specimens (the pure RTV-SR and the RTV-SR/OMMT-10) upon tensile shear testing starts with crack initiation. If the elastomeric network is capable of dissipating the input energy (*e.g.*, by converting into heat), then it can withstand higher stresses up to break. In the pure RTV-SR adhesive film, numerous voids appear during drawing, and cracks can be generated by the fillers *via* voiding. In the RTV-SR/OMMT-10 adhesive films, the nanoreinforcing effect caused by silicate layers may reduce the amount and size of voids in their vicinity and increase the length of the crack spread path around the silicate layers ("zig-zag" route), which can also be considered as a mechanism of energy dissipation. By this suggested

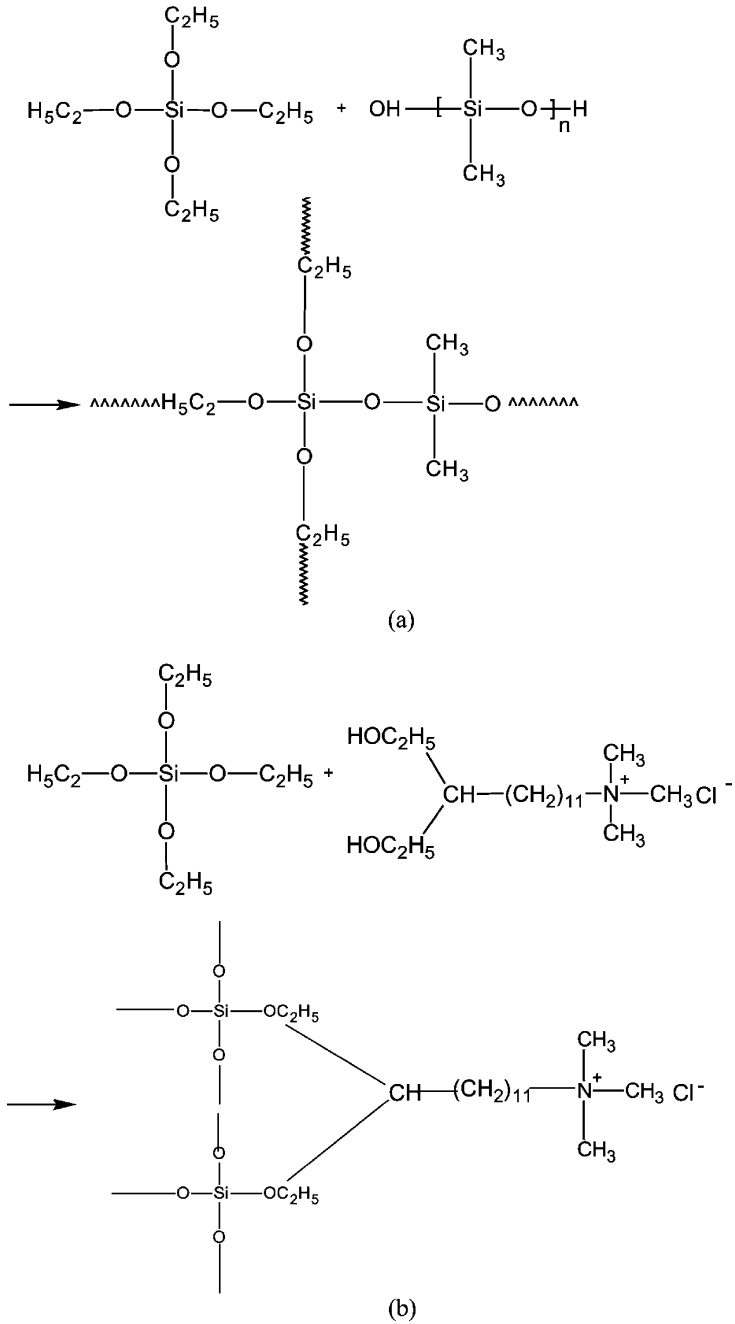

FIGURE 8 Schematic drawing of the intermolecular interactions: (a) two components of RTV-SR and (b) component B of RTV-SR and DDTAC.

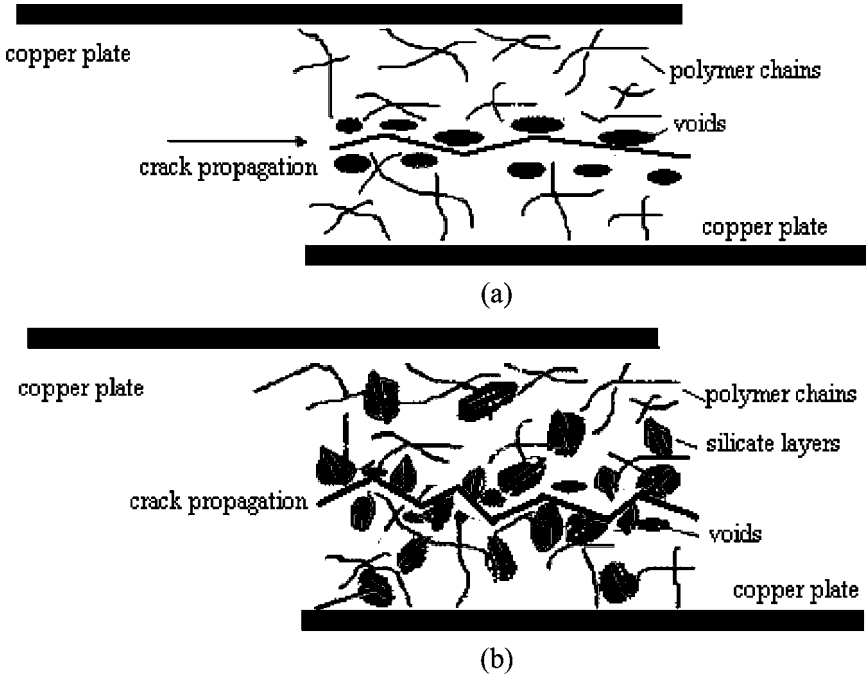

FIGURE 9 Scheme of the failure development: (a) pure RTV-SR adhesive and (b) RTV-SR/OMMT-10 adhesive.

model, the increase in cohesive strength and tensile properties seems to be normal for these clay-reinforced nanocomposites. Furthermore, the deterioration in the adhesive properties with increasing OMMT loading above a certain level can be explained by the onset of big agglomerates, which favors the initiation of catastrophic failure [33,34].

CONCLUSIONS

Novel RTV-SR/OMMT adhesives were successfully prepared by solution intercalation polymerization from a two-component RTV-SR and a new OMMT prepared by the intercalation agent, DDTAC.

The enhanced cohesive, tensile, and thermal properties of RTV-SR/OMMT demonstrated the efficient reinforcing and thermal stability properties of the OMMT.

FTIR, WAXD, and TEM results verified the effect of incorporating this OMMT into the RTV-SR matrix and revealed that the degree of

basal-spacing expansion was largely increased and a mixture of intercalated and exfoliated nanocomposites was formed.

A proposed cohesion mechanism for improved mechanical properties showed that the best cohesive property of RTV-SR/OMMT-10 adhesive was associated with good dispersion of the OMMT silicate layers and the resultant nanoeffect in the composite.

ACKNOWLEDGMENT

This work was financially supported by the Shanghai Leading Academic Discipline Project (p1402) and the Nanometer Special Project (0452NM080). The authors are thankful to Zhao Guangxian, the editor of the journal *of China Rubber Industry*, for helpful discussion.

REFERENCES

[1] Tsai, M. F., Lee, Y. D., and Ling, Y. C., *J. Appl. Polym. Sci.* **70**, 1669–1675 (1998).
[2] Zhao, S. G. and Feng, S. Y., *J. Appl. Polym. Sci.* **93**, 2095–2104 (2004).
[3] Wang, S., Xu, P., and Mark, J. E., *Rubber Chem. Technol.* **64**, 746–748 (1991).
[4] Yuan, Q. W. and Mark, J. E., *Macromol. Chem. Phys.* **20**, 206–209 (1999).
[5] Kohjiya, S. and Ikeda, Y., *Rubber Chem. Technol.* **73**, 534–526 (2000).
[6] Kohjiya, S., Murakami, K., and Iio, S., *Rubber Chem. Technol.* **74**, 16–19 (2001).
[7] Stöber, W., Fink, A., and Bohn, E. J., *J. Colloid Interface Sci.* **26**, 62–65 (1968).
[8] Kwan, K. S., Harrington, D. A., and Moore, P. A., *Rubber Chem. Technol.* **74**, 630–633 (2001).
[9] Arroyo, M., Lopez-Manchado, M. A., and Herrero, B., *Polymer* **44**, 2447–2451 (2003).
[10] Wang, Y. M., *Organosil. Mater. Appl. Chin.* **5**, 11–14 (1992).
[11] Wang, S. J., Li, Q., and Qi, Z. N., *Acta Polym. Sinica* **2**, 149–152 (1998).
[12] Wang, S. J., Long, C. F., Wang, X. Y., Li, Q., and Qi, Z., *J. Appl. Polym. Sci.* **69**, 1557–1560 (1998).
[13] Zhou, N. L., Xia, X. X., and Wang, Y. R., *Acta Polym. Sinica* **2**, 253–255 (2002).
[14] Younghoon, K. and James, L. W., *J. Appl. Polym. Sci.* **90**, 1583–1586 (2003).
[15] Zheng, H., Zhang, Y., Peng, Z. L., and Zhang, Y. X., *Polym. Polym. Composite* **12**, 3–7 (2004).
[16] Bray, H. J., Redfern, S. A., and Clark, S. M., *Mineral. Mag.* **62**, 647–650 (1998).
[17] Bala, P., Samantaray, B. K., and Srivastava, S. K., *Mater. Res. Bull.* **35**, 1717–1721 (2000).
[18] Oiphen, H. V. and Fripiat, J. J. (Eds.), *Handbook for Clay Materials and Other Nonmetallic Minerals* (Pergamon Press, Oxford, 2000).
[19] Yano, K., Usuki, A., and Okada, A. *J. Polym. Sci., Part A: Polym. Chem.* **31**, 2493–2496 (1993).
[20] Sheng, P. S., David, D. J., and Charles, A. W., *Polym. Degrd. Stab.* **84**, 274–277 (2004).
[21] Tortora, M. and Borrasi, G., *Polymer* **43**, 6147–6151 (2002).
[22] Chen, T. K., Tien, Y. I., and Wei, K. H., *Polymer* **41**, 1347–1350 (2000).
[23] Xu, R. J., Manias, E., Alan, J. S., and Runt, J., *Macromolecules* **34**, 338–341 (2001).
[24] Yao, K. J., Song, M., and Hourston, D. J., *Polymer* **43**, 1018 (2002).

[25] Konstantinos, G. G., Nikolaos, S. S., and Anton, A. A., *Macromol. Mater. Eng.* **289**, 1081–1084 (2004).
[26] Ma, J., Xu, J., and Ren, J. H., *Polymer* **44**, 4619 (2003).
[27] Chen, T. K., Tien, Y. I., and Wei, K. H., *J. Polym. Sci., Part A: Polym. Chem.* **37**, 2230–2233 (1999).
[28] Zhang, Z. J., Zhang, L. N., and Yang, L., *Polymer* **46**, 133–136 (2005).
[29] Alexandre, M. and Dubois, P., *Mater. Sci. Eng. R.* **28**, 1–5 (2000).
[30] Hachett, E., Manias, E., and Giannelis, E. P., *Chem. Mater.* **12**, 2161–2164 (2000).
[31] Bujdak, J., Hachett, E. P., and Giannelis, E. P., *Chem. Mater.* **12**, 2168–2170 (2000).
[32] Fu, X. and Qutubuddion, S., *Polymer* **42**, 807–811 (2001).
[33] Ganter, M., Gronki, W., Reichert, P., and Mulhaupt, R., *Rubber Chem. Technol.* **74**, 221–224 (2001).
[34] Mousa, A. and Karger-Kocsis, J., *Macromol. Mater. Eng.* **286**, 260–264 (2001).